Research Paper https://doi.org/10.7733/jnfcwt.2020.18.4.509

Investigating the Leaching Rate of $TiTe_3O_8$ Towards a Potential Ceramic Solid Waste Form

Hye Ran Noh[1,2,T], Dong Woo Lee[1,T], Kyungwon Suh[1], Jeongmook Lee[1], Tae-Hyeong Kim[1], Sang-Eun Bae[1,2], Jong-Yun Kim[1,2]*, and Sang Ho Lim[1,2,]*

[1]*Korea Atomic Energy Research Institute, 111, Daedeok-daero 989beon-gil, Yuseong-gu, Daejeon, Republic of Korea*

[2]*University of Science and Technology, 217, Gajeong-ro, Yuseong-gu, Daejeon, Republic of Korea*

[T]*These authors contributed equally to this work and are co-first authors*

(Received November 6, 2020 / Revised November 20, 2020 / Approved December 14, 2020)

An important property of glass and ceramic solid waste forms is processability. Tellurite materials with low melting temperatures and high halite solubilities have potential as solid waste forms. Crystalline $TiTe_3O_8$ was synthesized through a solid-state reaction between stoichiometric amounts of TiO_2 and TeO_2 powder. The resultant $TiTe_3O_8$ crystal had a three-dimensional (3D) structure consisting of TiO_6 octahedra and asymmetric TeO_4 seesaw moiety groups. The melting temperature of the $TiTe_3O_8$ powder was 820℃, and the constituent TeO_2 began to evaporate selectively from $TiTe_3O_8$ above around 840℃. The leaching rate, as determined using the modified American Society of Testing and Materials static leach test method, of Ti in the $TiTe_3O_8$ crystal was less than the order of 10^{-4} $g \cdot m^{-2} \cdot d^{-1}$ at 90℃ for durations of 14 d over a pH range of 2-12. The chemical durability of the $TiTe_3O_8$ crystal, even under highly acidic and alkaline conditions, was comparable to that of other well-known Ti-based solid waste forms.

Keywords: Solid waste form, Solid-state reaction, $TiTe_3O_8$, Leaching rate, Chemical durability

*Corresponding Author.
Jong-Yun Kim, Korea Atomic Energy Research Institute, E-mail: kjy@kaeri.re.kr, Tel: +82-42-868-4736
Sang Ho Lim, Korea Atomic Energy Research Institute, E-mail: slim@kaeri.re.kr, Tel: +82-42-868-2105

ORCID

Hye Ran Noh	http://orcid.org/0000-0003-0404-2542	Dong Woo Lee	http://orcid.org/0000-0003-3463-3743
Kyungwon Suh	http://orcid.org/0000-0003-3548-3535	Jeongmook Lee	http://orcid.org/0000-0002-3496-5965
Tae-Hyeong Kim	http://orcid.org/0000-0001-6483-5902	Sang-Eun Bae	http://orcid.org/0000-0003-2668-8950
Jong-Yun Kim	http://orcid.org/0000-0002-9165-0986	Sang Ho Lim	http://orcid.org/0000-0002-8583-5677

1. Introduction

The isolation of radioactive waste from the environment has been a critical concern for public health and safety. Since the first research on a new concept for vitreous or crystalline materials for the immobilization of radioactive waste was conducted in the 1950s, various glass waste forms have been studied for high-level radioactive wastes [1-3]. Amorphous borosilicate glass has been selected as a solid waste form in the past because, due to the unstructured molecular arrangement of glass, it can incorporate a wide range of chemical elements (*ca.* 20-30 elements). Other necessary properties such as waste loading, chemical durability, and processability for amorphous borosilicate glass are all reasonably acceptable for radioactive waste immobilization applications [4]. Thus, borosilicate glass has been used as a reference solid waste form for comparison of the performance characteristics. However, borosilicate glass is thermodynamically unstable and less resistant to leaching and weathering [5] than more stable crystalline ceramic waste forms currently in use. Various titanate-based (zirconolite, hollandite, perovskite, etc.), alumina-based (magnetoplumbite, nepheline, etc.), and silicate-based (pollucite, etc.) ceramic waste forms are advantageous over glass waste form equivalents [6,7]. These minerals exhibit various crystalline structures, such as fluorite, ABO_3, and ABO_4. A-site cations and B-site cations can be exchanged with fission product elements such as Cs, Rb, Sr, Ba, Th, and Pu [7-11].

Processing temperature and chemical durability are noteworthy properties when screening for a potential solid waste form. Processing temperature is an important property in terms of cost-effectiveness and secondary off-gas treatment for volatile radionuclides [6], while chemical durability is one of the most important performance characteristics of solid waste. There are several standard leach test protocols developed by the International Atomic Energy Agency (IAEA), the International Organization for Standardization (ISO), the American Society of Testing and Materials (ASTM), and American Nuclear Society (ANS). However, there is no single standard leach test method that can evaluate the performance of chemical durability under various field conditions of disposal facilities.

In this study, a chemical durability test was conducted based on the protocol described by ASTM C1220-17 [12] with some minor modifications of the experimental conditions. We identified the Ti^{4+}-Te^{4+}-oxide system for the immobilization of radioactive waste. $TiTe_3O_8$ is a potential Ti^{4+}-Te^{4+}-oxide because we anticipate that the replacement of cations in the crystal framework at the Ti^{4+} site with dopant cations can produce stable $Ti_{1-x}M_xTe_3O_8$ (M = Er^{3+}, Ce^{4+}, and Sn^{4+}) compounds [13-15]. In addition, a high quality solid solution between stoichiometric amounts of TiO_2 and TeO_2 is expected to be easily prepared through a simple solid-state reaction at 600-700℃.

2. Experimental

2.1 Solid-state synthesis of $TiTe_3O_8$

A polycrystalline sample of $TiTe_3O_8$ was prepared by the solid-state reaction of TiO_2 and TeO_2 powder. TiO_2 (Showa, 99.0%) and TeO_2 (Aldrich, 99.0%) were used as purchased without further purification. Stoichiometric amounts of TiO_2 and TeO_2 were thoroughly ground together in an agate mortar and pestle. After grinding, the reaction mixtures were pressed into pellets and transferred to an alumina crucible. The samples placed in the alumina crucible were heated to 650℃ at a rate of 5℃·min^{-1}, held at this temperature for 18 h for sintering, and cooled to room temperature at a rate of 5℃·min^{-1}.

2.2 Material characterization

Powder X-ray diffraction (XRD) analyses were conducted to examine the purity of the polycrystalline $TiTe_3O_8$ phase with a Bruker D8-Advance diffractometer using Cu Kα radiation at an operating voltage of 40 kV and a current

of 40 mA. The powder samples, which were prepared by grinding the pellet samples, were mounted on the sample holder, and measured in the 2θ range of 10-80° with a step size of 0.02° and a step time of 0.1 s. To investigate the thermal effects, the powder samples were heated at a rate of 10℃·min^{-1} up to the three different target temperatures of 300, 600, and 900℃. Each target temperature was maintained for 10 min and subsequently cooled to room temperature to measure the powder XRD patterns. The weight loss and melting temperature of the $TiTe_3O_8$ powder samples were measured by thermogravimetric analysis (TGA) and differential scanning calorimetry (DSC), respectively, using a SCINCO STA N-1500 TGA/DSC analyzer at a heating rate of 5℃·min^{-1} to 1,000℃ under a flow of argon gas.

After the leaching experiments, scanning electron microscopy (SEM) analyses were conducted on the pelletized samples using a JEOL JSM-6610LV scanning electron microscope to investigate any harmful effects on the crystalline structures and surface morphologies. XRD analysis was also performed for the pelletized samples after leaching under the same operating conditions as those for the powder samples.

2.3 Chemical durability test

The static leaching test method described by ASTM C1220-17 using deionized water was used to test the chemical durability of pelletized $TiTe_3O_8$ samples. High-purity deionized water is one of the most frequently employed aqueous solvents for leaching, as the appropriate pH and salt compositions of the aqueous leaching solution can be manipulated to simulate the specific groundwater conditions at the disposal sites. The 15-mm-diameter and 1.4-mm-thick pellets were immersed in 10 mL of deionized water. The acidity of the leaching solution spanned from an acidic solution (0.01 M HCl, pH=2) to an alkaline solution (0.01 M NaOH, pH=12). A 17 mL Teflon-lined, stainless steel autoclave containing the leaching solution and the pelletized sample was placed in a convection oven at 90℃ for 7 and 14 d. After 14 d, the concentration of the released Ti was measured by inductively coupled plasma-mass spectrometry (ICP-MS) using a iCAP TQ ICP-MS (Thermo Fisher Scientific) with the limit of detection (LOD) of 0.005 mg·L^{-1}.

Table 1. Crystallographic data of $TiTe_3O_8$ [16]

Empirical formula	$TiTe_3O_8$
Crystalline color	Yellow
Molecular mass (g·mol^{-1})	558.67
Crystal system	Cubic
Space group	*I a*-3 (No. 206)
Z	8
$a = b = c$ (Å)	10.9585(5)
V (Å^3)	1,315.99(10)
ρ_{calcd} (g·cm^{-3})	5.639

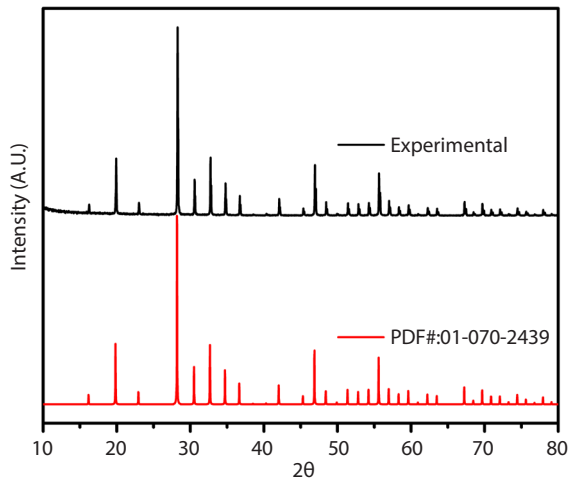

Fig. 1. Powder X-ray diffraction patterns of the solid-state synthesized $TiTe_3O_8$ powders (black line), and the reference structure of pure $TiTe_3O_8$ (red line, PDF#: 01-070-2439).

3. Results and discussion

3.1 Crystalline Structures

The incorporation of radionuclides into the crystalline framework of ceramic waste forms is key to the

Table 2. Atomic positions, site occupancies, and equivalent isotropic displacement parameters for $TiTe_3O_8$ [16]

Atom	x	y	z	Occupancy	U_{eq} [a]
Te(1)	0.0000	0.2500	0.21092(3)	1.0	0.00696(17)
Ti(1)	0.0000	0.0000	0.0000	1.0	0.0056(3)
O(1)	-0.1025(2)	0.4381(2)	0.3681(2)	1.0	0.01155(5)
O(2)	0.1736(2)	0.1736(2)	0.1736(2)	1.0	0.0077(7)

[a] U_{eq} ($Å^{-2}$) is defined as one-third of the trace of the orthogonalized U_{ij} tensor.

Table 3. Selected interatomic bond lengths and bond angles for $TiTe_3O_8$ [16]

Te-O	Bond length (Å)	O-Te-O	Bond angles (°)
Te(1) – O(1) × 2	1.884(2)	O(1) – Te(1) – O(1)	101.79(16)
Te(1) – O(2) × 2	2.1185(7)	O(1) – Te(1) – O(2) × 2	79.99(8)
Ti(1) – O(1) × 6	1.952(2)	O(1) – Te(1) – O(2) × 2	86.02(13)
		O(2) – Te(1) – O(2)	157.76(13)
		O(1) – Ti(1) – O(1) × 6	88.19(9)
		O(1) – Ti(1) – O(1) × 6	91.81(9)
		O(1) – Ti(1) – O(1) × 3	180.0(2)

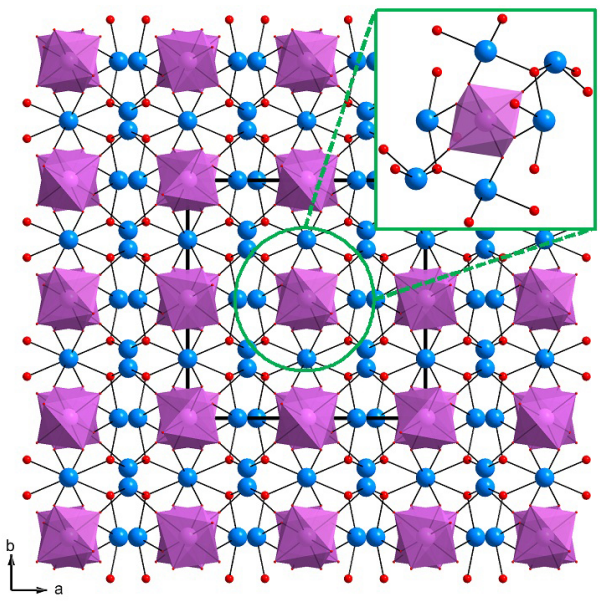

Fig. 2. Ball-and-stick representation of 3D structure of $TiTe_3O_8$ in *ab*-plane, TiO_6 octahedron and Te_3O_8 trimers by corner sharing of TeO_4 seesaw groups. The purple octahedrons represent TiO_6, the blue balls Te atoms, and the red balls O atoms.

immobilization of radioactive wastes. Fundamental information on crystalline structures is helpful for understanding waste form stability and incongruent dissolution. The reported values of crystallographic information, bond distances, and bond angles for crystalline $TiTe_3O_8$ are given in Tables 1-3 [16]. Fig. 1 shows that the powder X-ray diffraction pattern for $TiTe_3O_8$ powder prepared through solid-state sintering matched the polycrystalline $TiTe_3O_8$ (PDF#: 01-070-2439 in Fig. 1). No other impurities such as TiO_2 and TeO_2 phases were found in the sintered powders. As previous studies have shown [17], the crystal structure of $TiTe_3O_8$ showed the centrosymmetric cubic space group, *I a*-3 (No. 206). It reveals 3D frameworks consisting of TiO_6 octahedra and TeO_4 polyhedra (see Fig. 2). The unique Ti^{4+} cation is connected to six oxygen atoms in an octahedral coordination environment. The asymmetric unit indicated the presence of unique Te^{4+} cations, showing an unsymmetrical coordination moiety resulting from the

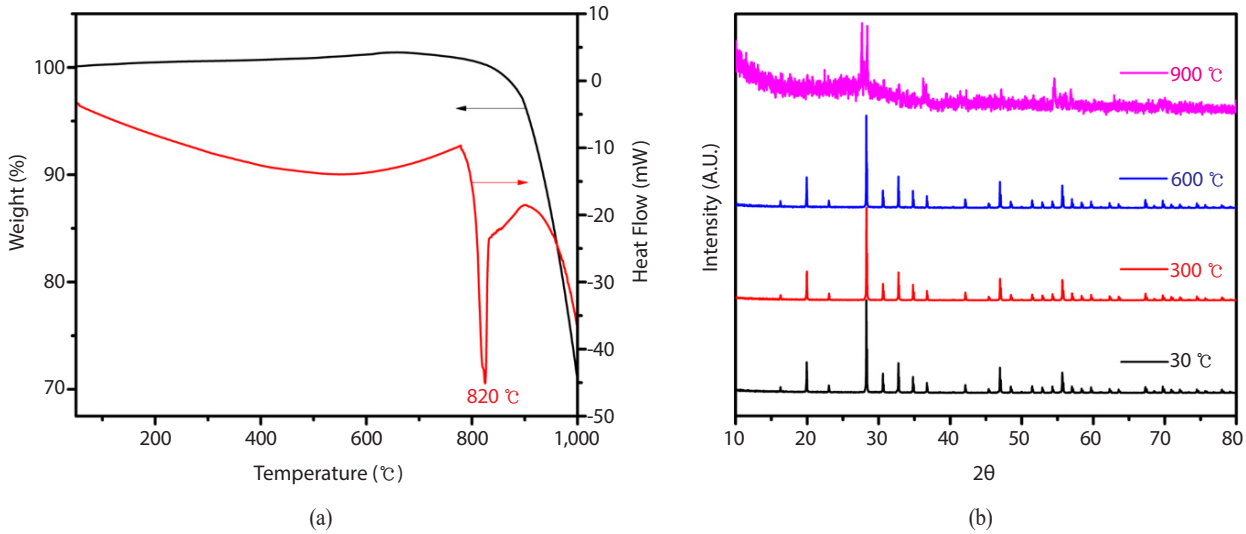

Fig. 3. Thermal behavior of $TiTe_3O_8$ powders. (a) Thermogravimetric analysis (black line), differential scanning calorimetry analysis (red line) data, and (b) X-ray diffraction patterns of $TiTe_3O_8$ powder treated at different temperatures for 10 min.

stereoactive lone pairs. The three distorted TeO_4 polyhedra share their corners through one O atom and form Te_3O_8 trimers. The Ti^{4+} cations in the center of the oxide octahedron are shared by two Te_3O_8 trimers in an asymmetric coordination environment. Each Te_3O_8 trimer is further connected by a TiO_6 octahedron along the [100] direction, thereby resulting in the formation of a 3D framework.

3.2 Thermal properties

TGA data showed that no significant weight loss of the synthesized $TiTe_3O_8$ powders was observed until the temperature reached the melting point of $TiTe_3O_8$, as shown in Fig. 3(a). The weight loss started at approximately 840℃, where the decomposition of $TiTe_3O_8$ took place. At 1,000℃, almost 30% of the total weight was evaporated from the $TiTe_3O_8$ powder. In the DSC analysis, an endothermic peak was observed at 820℃, which indicates the melting of $TiTe_3O_8$. To investigate the chemical behavior introduced by the TeO_2 volatilization on the $TiTe_3O_8$ melt, XRD patterns measured at room temperature were compared after heat treatments at different temperatures up to the volatilization temperature. Fig. 3(b) reveals that polycrystalline $TiTe_3O_8$ maintains crystallinity up to 600℃. However, it is evident from the XRD pattern of the sample heat-treated at 900℃ that an amorphous residue was formed after the selective evaporation of TeO_2 from the $TiTe_3O_8$ melt. Small XRD peaks also appeared, corresponding to the polycrystalline TiO_2 phase (PDF#: 21-1276) as well as polycrystalline TeO_2.

3.3 Chemical durability

Crystalline samples of pelletized $TiTe_3O_8$ were subjected to a static leach test. The leaching rate of $TiTe_3O_8$ was calculated using Eq. (2) from the normalized mass loss in Eq. (1) [12, 19].

$$NL_{Ti} = \frac{C_{Ti} \times V}{S \times f_{Ti}} \quad (1)$$

$$LR_{Ti} = \frac{NL_{Ti}}{t} \quad (2)$$

where NL_{Ti} is the normalized mass loss of Ti ($g \cdot m^{-2}$), LR_{Ti} is the leaching rate of Ti ($g \cdot m^{-2} \cdot d^{-1}$), C_{Ti} is the concentration of elemental Ti in the leaching solution ($g \cdot L^{-1}$), V is the volume of the leaching solution (L), f_{Ti} is the mass fraction of element Ti in the sample, S is the surface area

Table 4. Leaching rate of constituent Ti and Si element in various waste forms

Solid waste forms	Leaching rate (10^{-4} g·m^{-2}·d^{-1})	Melting point (℃)
Borosilicate glass	14,000 (Si) [18]	1,150 – 1,200 [6]
SYNROC	< 2 [20]	ca. 1,370 [24]
Perovskite	< 1 [21]	1,970 [25]
Hollandite	1,500 [22]	> 1,400 [25]
Pyrochlore	17 [23]	ca. 1,800 [26]

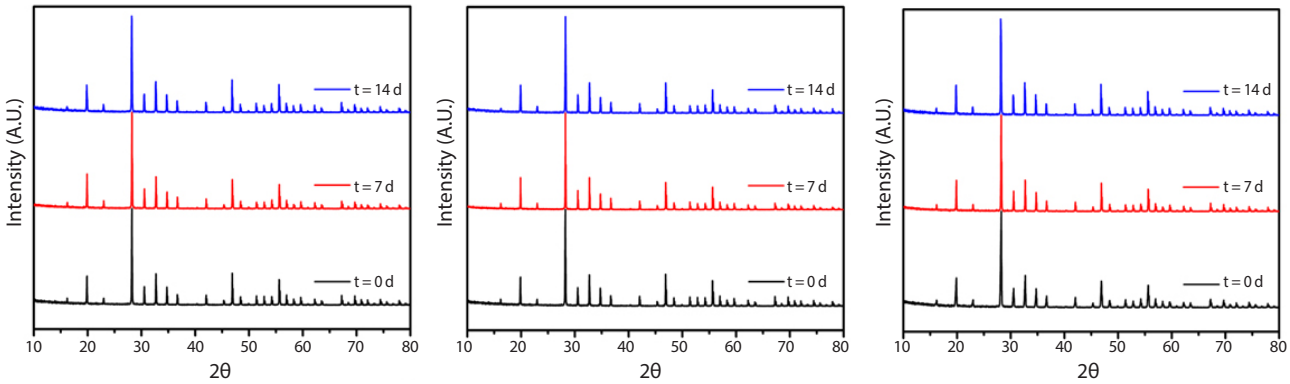

Fig. 4. XRD patterns of $TiTe_3O_8$ after leaching in (a) 0.01 M HCl aqueous solution, (b) pure deionized water, and (c) 0.01 M NaOH aqueous solution over t = 7 d (red line), 14 d (blue line), and XRD pattern of the sample before leaching (black line) as a reference.

of the sample (m^2), and t is the soaking time (d). All Ti concentrations in the leaching solutions of the 0.01 M HCl aqueous solution, pure deionized water, and 0.01 M NaOH aqueous solution were below the limit of detection (LOD). Based on the LOD values, LR_{Ti} under various leaching conditions in this study was less than the order of 10^{-4} g·m^{-2}·d^{-1}. The leaching rates of other titanate-based solid waste forms are shown in Table 4. The chemical durability of $TiTe_3O_8$ is comparable to that of known titanate-based solid waste forms, and is more stable than borosilicate glass, while the melting temperatures of titanate-based materials are higher than those of $TiTe_3O_8$. Because the high processing temperature can cause volatilization of radionuclides in waste, a low temperature process is advantageous in field practices.

The leaching rate of pelletized $TiTe_3O_8$ was low. Therefore, no changes were expected in the surface and crystal structure. The XRD results in Fig. 4 confirm that the crystal structures of $TiTe_3O_8$ remained unchanged after 7 and 14 d of leaching with highly acidic and alkaline aqueous solutions, as well as pure deionized water. SEM images also demonstrated that notable surface cracks or damages were not observed after leaching.

4. Conclusions

Pure crystalline $TiTe_3O_8$ powder was synthesized through the solid-state sintering reaction of stoichiometric amounts of TiO_2 and TeO_2 powder. The two most important and fundamental properties required for the nuclear waste immobilization, thermal stability, and chemical durability of

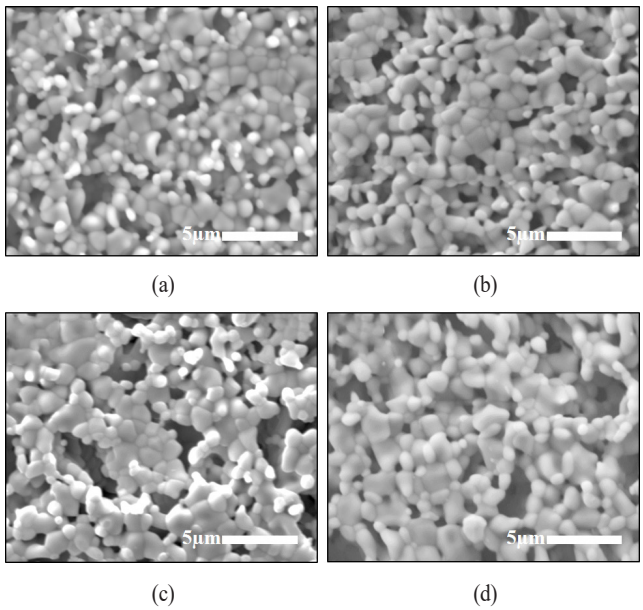

Fig. 5. SEM images of $TiTe_3O_8$ (a) before leaching and after leaching in (b) 0.01 M HCl aqueous solution, (c) pure deionized water, and (d) 0.01 M NaOH aqueous solution over 14 d.

$TiTe_3O_8$ were tested to examine the potential as a promising solid waste form. Although the $TiTe_3O_8$ melt became unstable at around 840°C, a thermally stable TiO_2 residue was formed after the volatilization of TeO_2 from $TiTe_3O_8$. The low melting temperature of the $TiTe_3O_8$ is advantageous in terms of cost, processability, and stability of wastes. The leaching rates of Ti in pelletized $TiTe_3O_8$ crystals were comparable to the well-known solid waste forms even under severe acidic and basic conditions. Further studies are required to investigate other important performance characteristics such as the loading capacity of fission products, mechanical strength, and radiation resistance.

Acknowledgements

This work was supported by the Nuclear Research and Development Program through the National Research Foundation of Korea (NRF-2017M2A8A5014754) funded by the Ministry of Science and ICT, Republic of Korea.

REFERENCES

[1] R. Eliassen and M.I. Goldman, "Disposal of High-Level Wastes by Fixation in Fused Ceramics", in: Industrial Radioactive Waste Disposal, Vol. 3, R.L. Doan, ed., 1966-1979, U.S. Government Printing Office, Washington, D.C. (1959).

[2] L.P. Hatch, "Ultimate Disposal of Radioactive Wastes", Am. Sci., 41(3), 410-421 (1953).

[3] D.R. Clarke, "Ceramic Materials for the Immobilization of Nuclear Waste", Annu. Rev. Mater. Sci., 13(1), 191-218 (1983).

[4] C.W. Kim and B.G. Lee, "Feasibility Study on Vitrification for Rare Earth Wastes of PyroGreen Process", J. Korean Radioact. Waste Soc., 11(1), 1-9 (2013).

[5] D.R. Clarke, "Preferential Dissolution of an Intergranular Amorphous Phase in a Nuclear Waste Ceramic", J. Am. Ceram. Soc., 64(6), c89-c90 (1981).

[6] National Research Council, Waste Forms Technology and Performance: Final Report, The National Academies Press, Washington D.C. (2011).

[7] A.I. Orlova and M.I. Ojovan, "Ceramic Mineral Wasteforms for Nuclear Waste Immobilization", Materials, 12(16), (2019).

[8] G.R. Lumpkin, "Ceramic Waste Forms for Actinides", Elements, 2(6), 365-372 (2006).

[9] M.L. Carter, E.R. Vance, D.R.G. Mitchell, J. V Hanna, Z. Zhang, and E. Loi, "Fabrication, Characterization, and Leach Testing of Hollandite, $(Ba,Cs)(Al,Ti)_2Ti_6O_{16}$", J. Mater. Res., 17(10), 2578-2589 (2002).

[10] Y. Zhang, M.W.A. Stewart, H. Li, M.L. Carter, E.R. Vance, and S. Moricca, "Zirconolite-rich Titanate Ceramics for Immobilisation of Actinides - Waste Form / HIP Can Interactions and Chemical Durability", J. Nucl. Mater., 395(1-3), 69-74 (2009).

[11] T.S. Livshits, J. Zhang, S.V. Yudintsev, and S.V. Stefanovsky, "New Titanate Matrices for Immobilization of REE-actinide High-level Waste", J. Radioanal. Nucl. Chem., 304(1), 47-52 (2015).

[12] ASTM C1220-17, "Standard Test Method for Static Leaching of Monolithic Waste Forms for Disposal of Radioactive Waste" (2017).

[13] I. Ayed, S. Elleuch, A. Ben Ahmed, and A. Kabadou, "Effect of Erbium Doping on Vibrational and Optical Properties of $TiTe_3O_8$", J. Alloys Compd., 791, 1088-1097 (2019).

[14] G. Nabila, R. Karray, J. Laval, A. Kabadou, and B.S. Abdelhamid, "X-ray Powder Diffraction and Raman Vibrational Study of New Doped Compound $TiTe_3O_8$:Ce", J. Mater. Environ. Sci., 6(4), 989-996 (2015).

[15] W. Ben Aribia, M. Loukil, A. Kabadou, and A. Ben Salah, "X-ray Powder Diffraction Study of $Sn_{0.59}Ti_{0.41}Te_3O_8$", Powder Diffr., 23(3), 228-231 (2008).

[16] W. Lu, Z. Gao, Q. Wu, X. Tian, Y. Sun, Y. Liu, and X. Tao, "Tailored Fabrication of a Prospective Acousto-optic Crystal $TiTe_3O_8$ Endowed with High Performance", J. Mater. Chem. C, 6(10), 2443-2451 (2018).

[17] J. Galy, G. Meunier, S. Andersson, and A. Åström, "Stéréochimie des Eléments Comportant des Paires Non Liées: Ge (II), As (III), Se (IV), Br (V), Sn (II), Sb (III), Te (IV), I (V), Xe (VI), Tl (I), Pb (II), et Bi (III) (Oxydes, Fluorures et Oxyfluorures)", J. Solid State Chem., 13(1), 142-159 (1975).

[18] D.M. Strachan, R.P. Turcotte, and B.O. Barnes, "MCC-1: A Standard Leach Test for Nuclear Waste Forms", Nucl. Technol., 56(2), 306-312 (1982).

[19] W.A. Ross, D.M. Strachan, R.P. Turcotte, and J.H.J. Westsik. Materials Characterization Center Workshop on Leaching of Radioactive Waste Forms. Summary Report, Battelle Pacific Northwest Laboratory Report, DOE-PNL-3318 (1980).

[20] D.M. Levins and R.S.C. Smart, "Effects of Acidification and Complexation from Radiolytic Reactions on Leach Rates of SYNROC C and Nuclear Waste Glass", Nature, 309, 776-778 (1984).

[21] R.G. Dosch, "Processing Effects on the Behavior of Titanate Waste Forms in Aqueous Solutions", Mater. Res. Soc. Symp. Proc., 6, 15-22 (1982).

[22] N. Kamel, F. Aouchiche, D. Moudir, Y. Mouheb, and S. Kamariz, "Study of the Chemical Durability of a Hollandite Mineral Leached in both Static and Dynamic Conditions", Environ. Res. Technol., 2(2), 85-92 (2019).

[23] Y.F. Volkov, S.V. Tomilin, A.N. Lukinykh, A.A. Lizin, A.A. Elesin, A.G. Yakovenko, V.I. Spiryakov, V.I. Konovalov, V.M. Chistyakov, A.V Bychkov, and L.J. Jardine, "Titanate Ceramics with Pyrochlore Structure as a Matrix for Immobilization of Excess Weapons-Grade Plutonium: II. Hydrolytic Resistance", Radiochemistry, 46(4), 358-363 (2004).

[24] A.E. Ringwood, V.M. Oversby, S.E. Kesson, W. Sinclair, N. Ware, W. Hibberson, and A. Major, "Immobilization of High-level Nuclear Reactor Wastes in SYNROC: A Current Appraisal", Nucl. Chem. Waste Manage., 2(4), 287-305 (1981).

[25] A.E. Ringwood, Safe Disposal of High Level Nuclear Reactor Wastes: a New Strategy, Australian National University Press, Canberra, Australia (1978).

[26] C.A. Taylor, "Helium Diffusion and Accumulation in $Gd_2Ti_2O_7$ and $Gd_2Zr_2O_7$", Ph.D. Dissertation, University of Tennessee (2016).